

Original Article



Inflammasome-Dependent Peroxiredoxin 2 Secretion Induces the Classical Complement Pathway Activation

Cheol Ho Park ^{1,2,†}, Hyun Sook Lee ^{1,3,†}, Man Sup Kwak ^{1,4}, Jeon-Soo Shin ^{1,3,4,5,*}

¹Department of Microbiology, Yonsei University College of Medicine, Seoul 03722, Korea

²Department of Internal Medicine, Institute of Kidney Disease Research, Yonsei University College of Medicine, Seoul 03722, Korea

³Brain Korea 21 Project for Medical Science, Yonsei University College of Medicine, Seoul 03722, Korea

⁴Institute for Immunology and Immunological Diseases, Yonsei University College of Medicine, Seoul 03722, Korea

⁵Severance Biomedical Science Institute, Yonsei University College of Medicine, Seoul 03722, Korea



Received: Jul 28, 2021

Revised: Aug 29, 2021

Accepted: Sep 8, 2021

*Correspondence to

Jeon-Soo Shin

Department of Microbiology, College of Medicine, Yonsei University, 50-1 Yonsei-ro Seodaemun-gu, Seoul 03722, Korea.
E-mail: jsshin6203@yuhs.ac

[†]Cheol Ho Park and Hyun Sook Lee contributed equally.

Copyright © 2021. The Korean Association of Immunologists

This is an Open Access article distributed under the terms of the Creative Commons Attribution Non-Commercial License (<https://creativecommons.org/licenses/by-nc/4.0/>) which permits unrestricted non-commercial use, distribution, and reproduction in any medium, provided the original work is properly cited.

ORCID iDs

Cheol Ho Park
<https://orcid.org/0000-0003-4636-5745>

Hyun Sook Lee
<https://orcid.org/0000-0003-2831-5402>

Man Sup Kwak
<https://orcid.org/0000-0002-3989-3016>

Jeon-Soo Shin
<https://orcid.org/0000-0002-8294-3234>

ABSTRACT

Peroxiredoxins (Prxs) are ubiquitously expressed peroxidases that reduce hydrogen peroxide or alkyl peroxide production in cells. Prxs are released from cells in response to various stress conditions, and they function as damage-associated molecular pattern molecules. However, the secretory mechanism of Prxs and their roles have not been elucidated. Thus, we aimed to determine whether inflammasome activation is a secretory mechanism of Prxs and subsequently identify the effect of the secreted Prxs on activation of the classical complement pathway. Using J774A.1, a murine macrophage cell line, we demonstrated that NLRP3 inflammasome activation induces Prx1, Prx2, Prx5, and Prx6 secretion in a caspase-1 dependent manner. Using HEK293T cells with a transfection system, we revealed that the release of Prx1 and Prx2 relies on gasdermin-D (GSDMD)-mediated secretion. Next, we confirmed the binding of both Prx1 and Prx2 to C1q; however, only Prx2 could induce the C1q-mediated classical complement pathway activation. Collectively, our results suggest that inflammasome activation is a secretory mechanism of Prxs and that GSDMD is a mediator of their secretion. Moreover, secreted Prx1 and Prx2 bind with C1q, but only Prx2 mediates the classical complement pathway activation.

Keywords: Peroxiredoxin 2; Inflammasome; Gasdermin D; Classical complement pathway

INTRODUCTION

Peroxiredoxins (Prxs) are a family of thiol peroxidases that scavenge peroxides, such as hydrogen peroxide and alkyl hydroperoxide, in cells. Mammals have 6 Prxs; Prx1, Prx2, and Prx6 are found in the cytoplasm; Prx3 in the mitochondria; Prx4 in the endoplasmic reticulum; and Prx5 in various cell compartments, including peroxisomes and mitochondria (1,2). Among these mammalian Prxs, studies have primarily focused on Prx1, Prx2, Prx3, and Prx4, and their antioxidative functions are well understood.

Conflict of Interest

The authors declare no potential conflicts of interest.

Abbreviations

AIM2, absent in melanoma 2; BMDM, bone marrow-derived macrophage; DAMP, damage-associated molecular pattern; GSDMD, gasdermin-D; HEK, human embryonic kidney; HMGB1, high-mobility group box 1; KO, knock-out; MAC, membrane attack complex; NHS, normal human serum; NLR4, nucleotide-binding oligomerization domain-like receptor containing a caspase recruitment domain 4; NLRP3, Nod-like receptor family pyrin domain containing 3; OD, optical density; Prx, peroxiredoxin; RT, room temperature; TBS, Tris-buffered saline; TMB, tetramethylbenzidine; WCL, whole-cell lysate.

Author Contributions

Conceptualization: Park CH, Lee HS, Kwak MS, Shin JS; Funding acquisition: Kwak MS, Shin JS; Investigation: Park CH, Lee HS, Kwak MS; Methodology: Park CH, Lee HS, Kwak MS, Shin JS; Supervision: Shin JS; Validation: Shin JS; Writing- original draft: Park CH, Lee HS; Writing- review & editing: Park CH, Shin JS.

Prxs scavenge peroxides that damage DNA, RNA, or proteins in cells, revealed by experiments using Prx1- or Prx2-deficient mice (3-5). Although the intracellular function of Prxs is well understood, few studies focused on the extracellular functions of Prxs. Shichita et al. (6), using a mouse focal brain ischemia model, have reported that Prxs are released from necrotic brain tissues; the released Prxs mediate the secretion of inflammatory cytokines, and the amount of the released Prxs correlate with the infarct volume. Salzano et al. (7) reported that LPS stimulate the secretion of Prx2 from macrophages, and the released Prx2 induces the secretion of inflammatory cytokines. Recently, He et al. (8) reported that circulating Prx1 promoted inflammation in a mouse acetaminophen-induced acute liver injury model. The aforementioned findings suggest that extracellular Prxs function as damage-associated molecular pattern (DAMP) molecules. However, the secretion mechanism of Prxs remains unclear.

Inflammasomes are molecular platforms that are activated upon cellular infection or stress. They trigger the activation of caspase-1 and maturation of proinflammatory cytokines, such as IL-1 β and IL-18, to engage in innate immune defenses (9). Activated caspase-1 cleaves gasdermin-D (GSDMD) and liberates the N-terminal effector domain of GSDMD (N-GSDMD); consequently, N-GSDMD oligomerizes at the cell membrane and forms a pore through which small molecules, including IL-1 β , IL-18, high-mobility group box-1 (HMGB1), and DNA, are secreted (10). Since the diameter of the GSDMD pore is 10–16 nm (11,12), various intracellular components with a size comparable to that of the molecules secreted through the GSDMD pore could be secreted in this manner.

The complement system—a component of the innate immune system—acts as a first-line defense mechanism against pathogens and a sensor for altered self-molecules through three activation pathways: classical, alternative, and lectin (13,14). Conventionally, it is well accepted that the binding of C1q initiates the classical complement pathway to IgM or IgG in immune complexes, various pathogen-associated molecular pattern molecules, or apoptotic cell debris (15,16). We recently reported that HMGB1, a DAMP molecule released upon cell necrosis or tissue damage, can activate the classical complement pathway and contribute to sterile inflammation. These findings suggest that various DAMP molecules are candidates for triggering the activation of the classical complement pathway (17).

Here, we demonstrate that activation of various inflammasomes such as Nod-like receptor (NLR) family pyrin domain containing 3 (NLRP3), nucleotide-binding oligomerization domain-like receptor containing a caspase recruitment domain 4 (NLR4), and absent in melanoma 2 (AIM2), triggers the release of Prxs from macrophages in a caspase-1 dependent manner, using molecular studies and a cell culture model system; we identified that GSDMD was a possible route of Prx secretion, using a transfection system; and we showed that C1q bound with extracellular Prx1 and Prx2, wherein Prx2 and not Prx1 activated the classical complement pathway in an Ab-independent manner, using molecular studies and confocal microscopy. Collectively, our results suggest that inflammasomes possibly mediate the release of Prx2 from macrophages, and the released Prx2 was an Ab-independent binding partner of C1q that activated the classical complement pathway.

MATERIALS AND METHODS

Cell cultures

Cells from a murine macrophage cell line, J774A.1 (ATCC, Manassas, VA, USA), were cultured in RPMI 1640 medium supplemented with 10% heat-inactivated FBS, 100 µg/ml penicillin, 100 U/ml streptomycin, and 2 mM L-glutamine at 37°C under humidified 5% CO₂. In addition, human embryonic kidney (HEK) 293T (ATCC) cells were cultured in DMEM supplemented with the aforementioned reagents at 37°C under humidified 5% CO₂.

Bone marrow-derived macrophage (BMDM) preparation

Wild-type or NLRP3 knock-out (KO) C57BL/6 mice were obtained from OrientBio (Seongnam, Korea) and The Jackson Laboratory (Bar Harbor, ME, USA), respectively. The mice were housed in a specific-pathogen-free-grade facility with a 12:12-h light:dark cycle and fed with standard diet and tap water *ad libitum* under controlled room temperature (RT, 22°C±1°C) and humidity (50%±5%) in the animal facility of Yonsei University. All animal protocols were approved by the Institutional Animal Care and Use Committees of Yonsei University (2015-0275). For all experiments, 8-wk-old female mice (20±1.5 g body weight) were used. The animals were euthanized, and their femur and tibia were extracted. Bone marrow was collected via warm, serum-free DMEM lavage until no remaining bone marrow was visible. Bone marrow was collected and filtered through a 40-µm-pore cell strainer (SPL, Pocheon, Korea) and then washed with excessive media to ensure the removal of all debris.

The cells were then plated onto a 100-mm cell culture-treated dish and differentiated using 20 ng/ml mG-CSF (R&D systems, Minneapolis, MN, USA) in a complete medium for 7 days to yield BMDMs.

Induction of Prx secretion from cells

To trigger conventional NLRP3 inflammasome activation, J774A.1 cells were primed with 0.25 µg/ml LPS (Sigma-Aldrich, St. Louis, MO, USA) for 3 h and then treated with 2.5 mM ATP (Sigma-Aldrich) for 30 min with or without 10 µM Y-VAD (InvitroGen, Carlsbad, CA, USA), a selective caspase-1 inhibitor. To induce NLRC4 or AIM2 inflammasome, J774A.1 cells were primed as described above and then transfected with 0.5 µg/ml flagellin (InvitroGen) or 1 µg/ml poly(dA:dT) (InvitroGen) for 3 h, using Lipofectamine 2000 (InvitroGen) according to the manufacturer's protocol.

Flag-tagged caspase-11 (Flag-Caspase-11) and either Flag-tagged wild-type GSDMD (Flag-GSDMD [WT]) or D276A mutant GSDMD (Flag-GSDMD [D276A]) were transfected into HEK293T cells. Flag-GSDMD (D276A) was constructed in our laboratory. Then, HEK293T cells were treated with 20 µg/ml LPS for 4 h with or without 10 µM Z-VAD (InvitroGen), a pan-caspase inhibitor. Alternatively, HEK293T cells were transfected with Flag-tagged wild-type C-terminal domain of GSDMD (Flag-GSDMD-CT [WT]), wild-type N-terminal domain of GSDMD (Flag-GSDMD-NT [WT]), or 4A mutant N-terminal domain of GSDMD (Flag-GSDMD-NT [4A]) and cultured for 48 h.

Immunoblot analysis

J774A.1, HEK293T, or BMDM cells were washed with PBS and lysed in 1 X RIPA buffer (GenDEPOT, Katy, TX, USA) containing 150 mM NaCl, 1% Triton X-100, 1% deoxycholic acid sodium salt, 0.1% SDS, 50 mM Tris-HCl pH 7.5, 2 mM EDTA, and protease inhibitor cocktail (GenDEPOT). Whole-cell lysates (WCLs) were centrifuged at 20,000 *g* (4°C, 15 min) and

protein sample buffer (100 mM Tris-HCl pH 6.8, 2% SDS, 25% glycerol, 0.1% bromophenol blue and 5% β -mercaptoethanol) was added, followed by heating at 94°C for 5 min. Protein concentration was estimated using the BCA Protein Assay Kit (Thermo Fisher Scientific, Waltham, MA, USA). Equal amounts of proteins were loaded in each gel lane and separated by SDS-PAGE. The cell culture supernatants were collected, and proteins were precipitated by adding methanol and chloroform mixture as described in a previous study (18), followed by the addition of a protein sample buffer and heating as described above; the samples were loaded in individual lanes and separated by SDS-PAGE. After transferring to nitrocellulose membranes (GE Healthcare, Chicago, IL, USA), non-specific binding sites were blocked by incubating the membranes in Tris-buffered saline (TBS) supplemented with 0.1% Tween 20 and 5% (w/v) low-fat milk at RT for 1 h. Anti-Prx1, anti-Prx3, anti-Prx4, anti-Prx5, anti-Prx6 (AbFrontier, Seoul, Korea), anti-Prx2 (Abcam, Cambridge, UK), anti-caspase-1, anti-NLRP3 (Adipogen, San Diego, CA, USA), anti-IL-1 β (R&D systems), anti-C5b-9 (Quidel, San Diego, CA, USA), and anti- β -actin (Cell Signaling Technology, Danvers, MA, USA) Abs were used. The membranes were washed three times for 10 min with TBS supplemented with 0.1% Tween[®] 20 and probed with the appropriate HRP-conjugated secondary Abs (Jackson ImmunoResearch, West Grove, PA, USA) at RT for 1 h. After washing thrice, an enhanced chemiluminescence substrate was used for visualization. The membranes were then stripped by submerging in EzReprobe (ATTO Corporation, Tokyo, Japan) at RT for 30 min.

ELISA analysis

The binding of Prx1 or Prx2 with C1q was tested using ELISA. A microtiter plate (Corning Costar, Corning, NY, USA) was coated with 1 μ g/ml of human Prx1 (hPrx1), human Prx2 (hPrx2), mouse Prx1 (mPrx1), or mouse Prx2 (mPrx2) per well and blocked with 3% BSA-PBS. All these recombinant proteins were obtained from the laboratory of Prof. Sue Goo Rhee (Yonsei University, Seoul, Korea). Various concentrations of recombinant C1q (Sigma-Aldrich) in PBS were added to the wells and incubated at RT for 2 h. After washing, rabbit anti-C1q Ab (Dako, Glostrup, Denmark) and HRP-conjugated anti-rabbit Ig (Jackson ImmunoResearch) were added. Subsequently, 3,3',5,5'-tetramethylbenzidine (TMB) solution (Kirkegaard & Perry Laboratories, Gaithersburg, MD, USA) was used for color development for 15 min. Optical density values were measured at 450 nm.

Complement activation assay

To test classical complement pathway activation triggered by the binding of C1q to either Prx1 or Prx2, a microtiter plate was coated with 1 μ g/ml hPrx1, hPrx2, mPrx1, or mPrx2 per well and blocked with 3% BSA-PBS. Normal human serum (NHS), prepared in our laboratory and preserved at -70°C, was diluted in veronal-buffered saline (Lonza, Walkersville, MD, USA) and added to the wells at 37°C for 20 min or 45 min to measure C4b or C5b-9 deposition, respectively. After washing with PBST at 4°C, the cells were incubated with anti-C4b Ab (Dako) or anti-C5b-9 Ab (Quidel) at 37°C for 1 h and then probed with appropriate HRP-conjugated secondary Abs at RT for 1 h. After washing with PBST, a TMB solution was used for color development for 15 min. Optical density values were measured at 450 nm. To delineate whether Prx2 activated the complement pathway in a C1q-dependent manner, a microtiter plate was coated with 1 μ g/ml hPrx2 per well and blocked with 3% BSA-PBS. A C1q-depleted human serum (Quidel) or C1q-depleted human serum supplemented with C1q was diluted in veronal-buffered saline and added to the wells at 37°C for 45 min to measure the C5b-9 deposition. After performing all the aforementioned procedures, the optical density values were measured at 450 nm. To identify C5b-9 accumulation on the cell surface following complement activation mediated by hPrx2, J774A.1 cells were incubated in serum-

free RPMI 1640 medium, and 10% NHS and 5 µg/ml hPrx2 were added. After 2 h, the culture supernatants were removed, and WCLs were processed and analyzed by immunoblot assay as described above.

Complement consumption assay

Complement consumption assay was performed using the protocol described in previous studies (19,20). The consumption of human hemolytic complement by hPrx2 was calculated from the quantitative assay of residual CH₅₀ in NHS after reaction with various concentrations of hPrx2. Briefly, diluted NHS (CH₅₀) was incubated with various quantities of hPrx2 at 37°C for 30 min. Afterward, Ab-sensitized sheep erythrocytes were added, and the mixture was incubated at 37°C for 30 min. To stop the reaction, 4°C veronal-buffered saline was added. Supernatants were harvested after centrifugation, and absorption values were determined at 405 nm. Relative complement consumption was calculated using the following formula:

$$\text{Relative complement consumption (\%)} = \left[1 - \frac{\text{OD}_{\text{sample}} - \text{OD}_{\text{spontaneous hemolysis}}}{\text{OD}_{\text{hemolysis by normal human serum}} - \text{OD}_{\text{spontaneous hemolysis}}} \right] \times 100,$$

where OD refers to optical density.

Confocal microscopy

C3c accumulation following complement pathway activation was observed under confocal microscopy. J774A.1 cells were plated on Lab-Tak™II 8-well chambers (Thermo Fisher Scientific), and the culture medium was changed to serum-free RPMI 1640. The cells were incubated with 1 or 5 µg/ml hPrx2 in 10% NHS at 37°C for 2 h. After removing the culture supernatant, the cells were fixed with 4% paraformaldehyde (Biosesang, Seongnam, Korea) in PHEM buffer at RT for 30 min and washed with 4°C PBS. After blocking with 1% BSA-PBS at RT for 1 h, the cells were reacted with mouse anti-C3c-FITC Ab (Abcam) at RT for 2 h and then stained with DAPI (Vector Laboratories, Burlingame, CA, USA). Using FV1000 confocal microscopy (Olympus Optical, Tokyo, Japan), C3c accumulated on the cell surface was observed.

Statistical analysis

For immunoblot analysis, films were scanned, and the band density was determined using a densitometer and the image analysis software ImageJ (Version 1.53; National Institutes of Health, Bethesda, MD, USA). Analysis of all experimental data was performed by either Student's *t*-test or one-way ANOVA using GraphPad Prism (Version 9.0.0; GraphPad Software, San Diego, CA, USA). Data are represented as their mean value and standard error of the mean, as indicated in individual figure legends. Statistical differences were considered significant at *p*<0.05.

RESULTS

Inflammasomes mediate Prx secretion from murine macrophages in a caspase-1 dependent manner

Inflammasome activation leads to caspase-1 activation and results in pore formation at the plasma membrane, allowing the secretion of various intracellular molecules (9,10). To examine whether inflammasomes activation could mediate the secretion of Prxs from macrophages

Prx 2 Induces the Classical Complement Pathway Activation

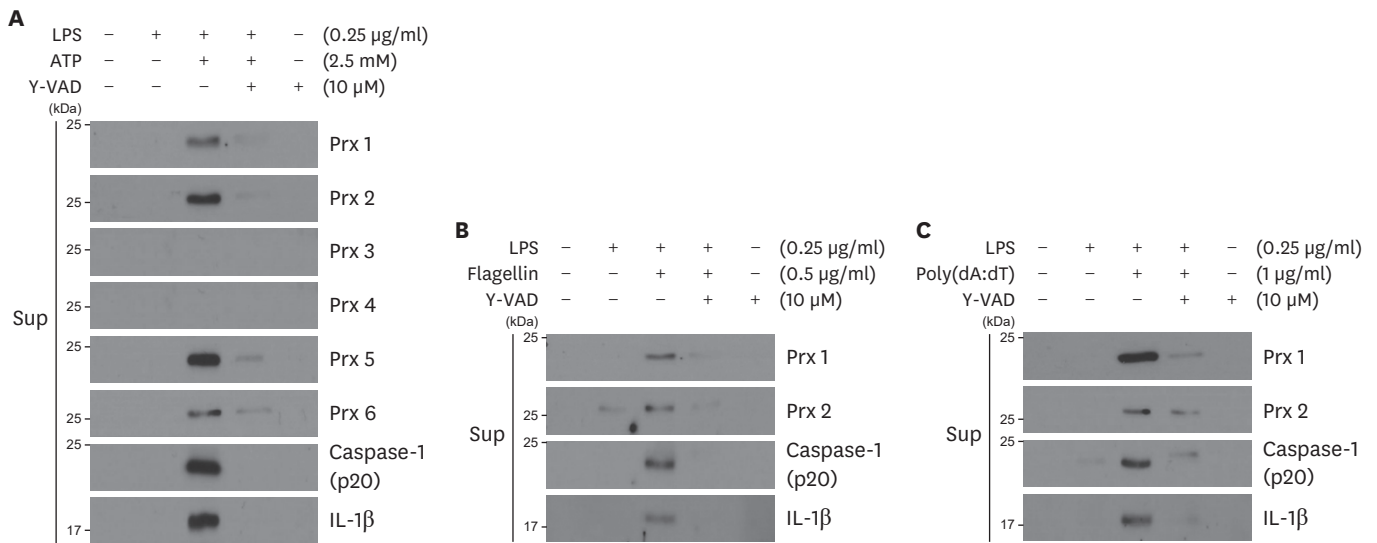


Figure 1. Inflammasomes mediate Prx secretion from murine macrophages in a caspase-1-dependent manner. J774A.1 cells were primed with 0.25 µg/ml LPS for 3 h; then, they were treated with 2.5 mM ATP for 30 min (A) or transfected with either 0.5 µg/ml flagellin (B) or 1 µg/ml poly(dA:dT) for 3 h (C) in the absence or presence of 10 µM Y-VAD. Supernatants (Sup) were subjected to SDS-PAGE and immunoblotting.

and whether the secretion of Prxs was dependent on caspase-1, we stimulated J774A.1 cells with LPS and ATP in the absence or presence of Y-VAD, a selective caspase-1 inhibitor, and observed the secretion of various Prxs by immunoblotting the culture supernatants of the cells (**Fig. 1A**). Among the 6 Prx subtypes, Prx1, Prx2, Prx5, and Prx6 were detected in the culture supernatants upon NLRP3 inflammasome activation in a caspase-1-dependent manner, whereas Prx3 and Prx4 were not secreted upon such stimulation. Since Prx1 and Prx2 act as DAMP molecules among the various Prxs (7,8), we focused on Prx1 and Prx2 in the subsequent experiments. We observed that NLRP3 inflammasome activation induced the secretion of Prx1 and Prx2 in BMDMs (**Supplementary Fig. 1A**). Other stimuli, such as LPS+nigericin or LPS+alum, that induce NLRP3 inflammasome activation also induced Prx2 secretion in J774A.1 cells (**Supplementary Fig. 1B**). Furthermore, using NLRP3-deficient BMDMs, we observed that Prx2 secretion induced by LPS/ATP occurred in an NLRP3 inflammasome-dependent manner (**Supplementary Fig. 1C**). Next, we examined the possibility that NLRC4 and AIM2 inflammasome activation also triggered the secretion of Prx1 and Prx2 in a caspase-1-dependent manner. We stimulated J774A.1 cells with LPS and either flagellin or poly(dA:dT) to activate NLRC4 or AIM2 inflammasome, respectively, in the absence or presence of Y-VAD; then, we observed the secretion of Prx1 and Prx2 (**Fig. 1B and C**). Similar to the NLRP3 inflammasome activation, NLRC4 (**Fig. 1B**) and AIM2 (**Fig. 1C**) inflammasome activation also induced the secretion of Prx1 and Prx2 in a caspase-1-dependent manner.

Release of Prx1 and Prx2 is dependent on GSDMD-mediated secretion

Next, we evaluated the role of GSDMD in the secretion of Prx1 and Prx2 with HEK293T cells using a transfection system. Various inflammatory caspases activated during inflammasome activation cleave GSDMD and liberate N-GSDMD; the liberated N-GSDMD oligomerizes at the cell membrane and forms a pore (10). Inflammatory caspases recognize the linker domain of GSDMD, and oligomerization of N-GSDMD is mediated by its aspartic acid motif; thus, we transfected HEK293T cells with different expression vectors. To analyze the effect of the non-cleaved form of GSDMD and the effect of the non-pore forming form of GSDMD, Flag-GSDMD (D276A) and Flag-GSDMD-NT (4A) were used, respectively (**Fig. 2A**)

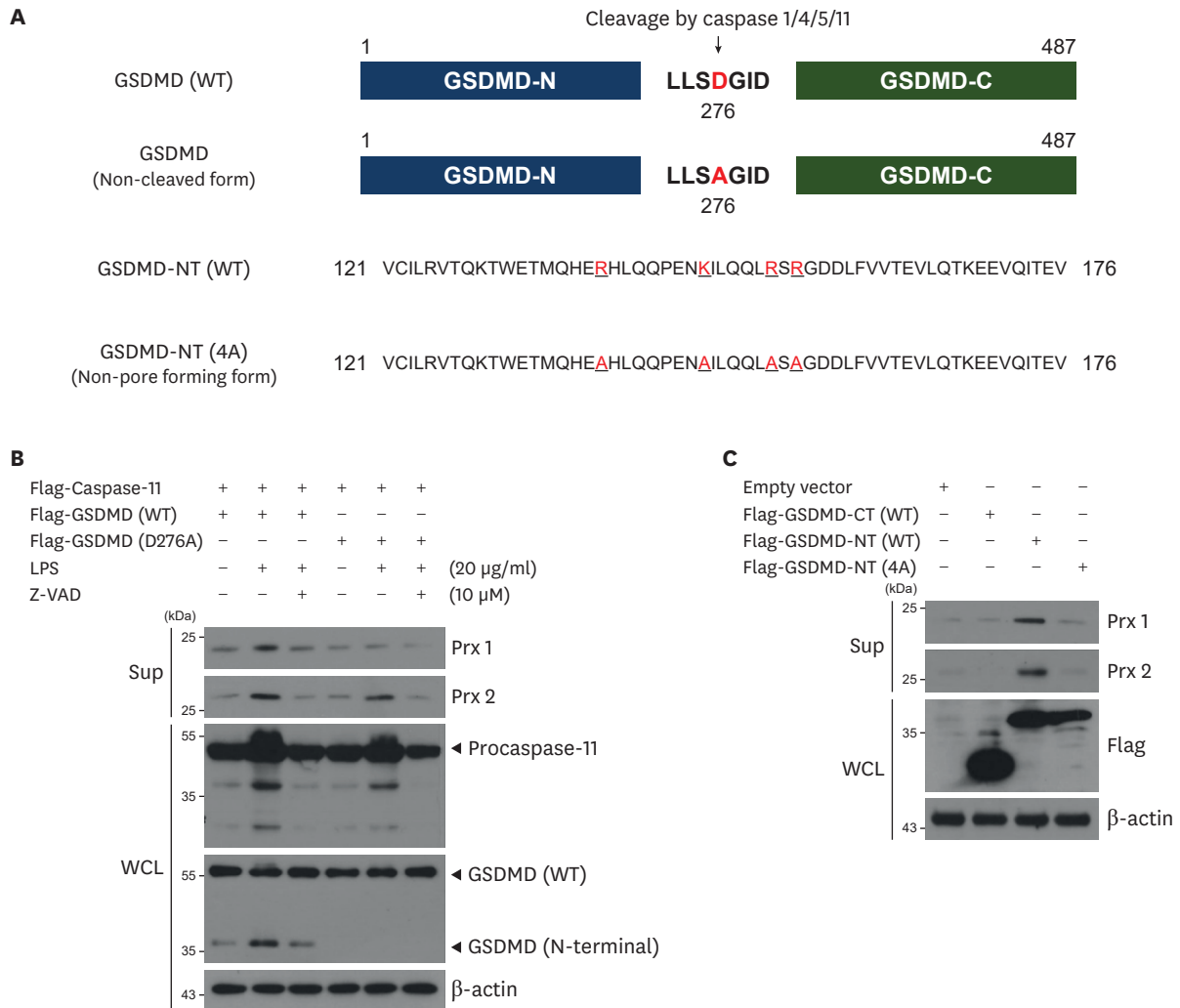


Figure 2. Release of Prx1 and Prx2 is dependent on GSDMD-mediated secretion. (A) Diagram of GSDMD structures that used in the experiments. (B) HEK293T cells were transfected with Flag-Caspase-11 and Flag-GSDMD (WT) or Flag-GSDMD (D276A) and stimulated with 20 µg/ml LPS for 4 h in the absence or presence of 10 µM Z-VAD. Sup and WCLs were subjected to SDS-PAGE and immunoblotting. (C) HEK293T cells were transfected with Flag-GSDMD-CT (WT), Flag-GSDMD-NT (WT), or Flag-GSDMD-NT (4A). Sup and WCLs were subjected to SDS-PAGE and immunoblotting.

(12,21-23). In the Flag-GSDMD (WT)-transfected HEK293T cells, caspase-11 activation upon LPS transfection showed the secretion of Prx1 and Prx2 in a caspase-11-dependent manner. However, in Flag-GSDMD (D276A)-transfected HEK293T cells, caspase-11 activation upon LPS transfection showed reduced secretion of Prx1 and Prx2 compared with that in Flag-GSDMD (WT)-transfected HEK293T cells (**Fig. 2B**). In Flag-GSDMD-CT (WT)-transfected HEK293T cells, Prx1 and Prx2 were rarely detected in the culture supernatants, whereas Flag-GSDMD-NT (WT)-transfected HEK293T cells (wherein N-GSDMD spontaneously oligomerized and formed pores at the plasma membrane) showed remarkable Prx1 and Prx2 secretion. However, in Flag-GSDMD-NT (4A)-transfected HEK293T cells, in which N-GSDMD could not oligomerize and form pores at the plasma membrane, showed reduced secretion of Prx1 and Prx2 (**Fig. 2C**).

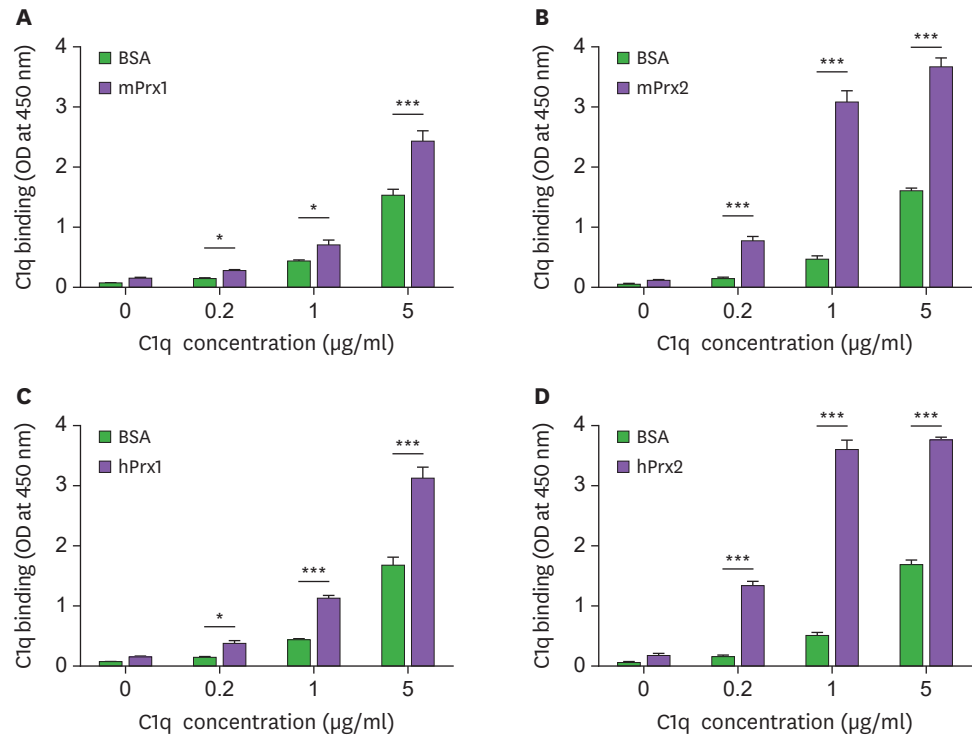


Figure 3. Prx1 and Prx2 are bound to C1q. (A-D) Recombinant mPrx1, mPrx2, hPrx1, or hPrx2 proteins (1 µg/ml) were immobilized on a microtiter plate, and different concentrations of C1q were added for performing ELISA. A blank was used as a negative control. Data are expressed as means±SEMs (n=3). *p<0.05, ***p<0.001 as Student's paired *t*-test.

Prx1 and Prx2 are bound to C1q

Next, we investigated the binding capacity of Prx1 and Prx2 with C1q to elucidate the possibility that secreted Prx1 or Prx2 could activate the classical complement pathway. Thus, investigating the binding capacity of Prx1 or Prx2 with C1q could be useful to explore this possibility. To determine whether Prx1 or Prx2 is bound to C1q, microtiter plates were coated with mPrx1, mPrx2, hPrx1, or hPrx2, and binding of C1q with various forms of Prx1 or Prx2 was measured using ELISA (Fig. 3A-D). We observed that C1q bound with mPrx1, mPrx2, hPrx1, and hPrx2 in a concentration-dependent manner. (Fig. 3A-D).

Binding of Prx2 to C1q activates the classical complement pathway

C1q is the initial component of the classical complement pathway activation, and it induces the cleavage of C4 to C4b. Thus, we measured C4b deposition using ELISA after adding an increasing concentration of NHS on mPrx1, mPrx2, hPrx1, or hPrx2-coated plates; anti-C4b was added to verify whether cleavage of C4 is induced by the binding of Prx1 or Prx2 to C1q. We observed that mPrx2 and hPrx2 induced C4b deposition; mPrx1 and hPrx1 induced C4b deposition insufficiently (Fig. 4A). Next, we observed C5b-9 deposition, known as a membrane attack complex (MAC) and the final effector of the complement system, using ELISA. Increasing concentrations of NHS were added to mPrx1, mPrx2, hPrx1, or hPrx2-coated plates, and anti-C5b-9 Ab was added to monitor the accumulation of C5b-9. Consequently, we observed that mPrx2 and hPrx2 induced C5b-9 deposition in an NHS concentration-dependent manner; however, mPrx1 and hPrx1 failed to induce C5b-9 deposition (Fig. 4B). C3c (a cleaved form of C3b) is another product of the complement pathway activation. We observed its accumulation on the cell surface using confocal

Prx 2 Induces the Classical Complement Pathway Activation

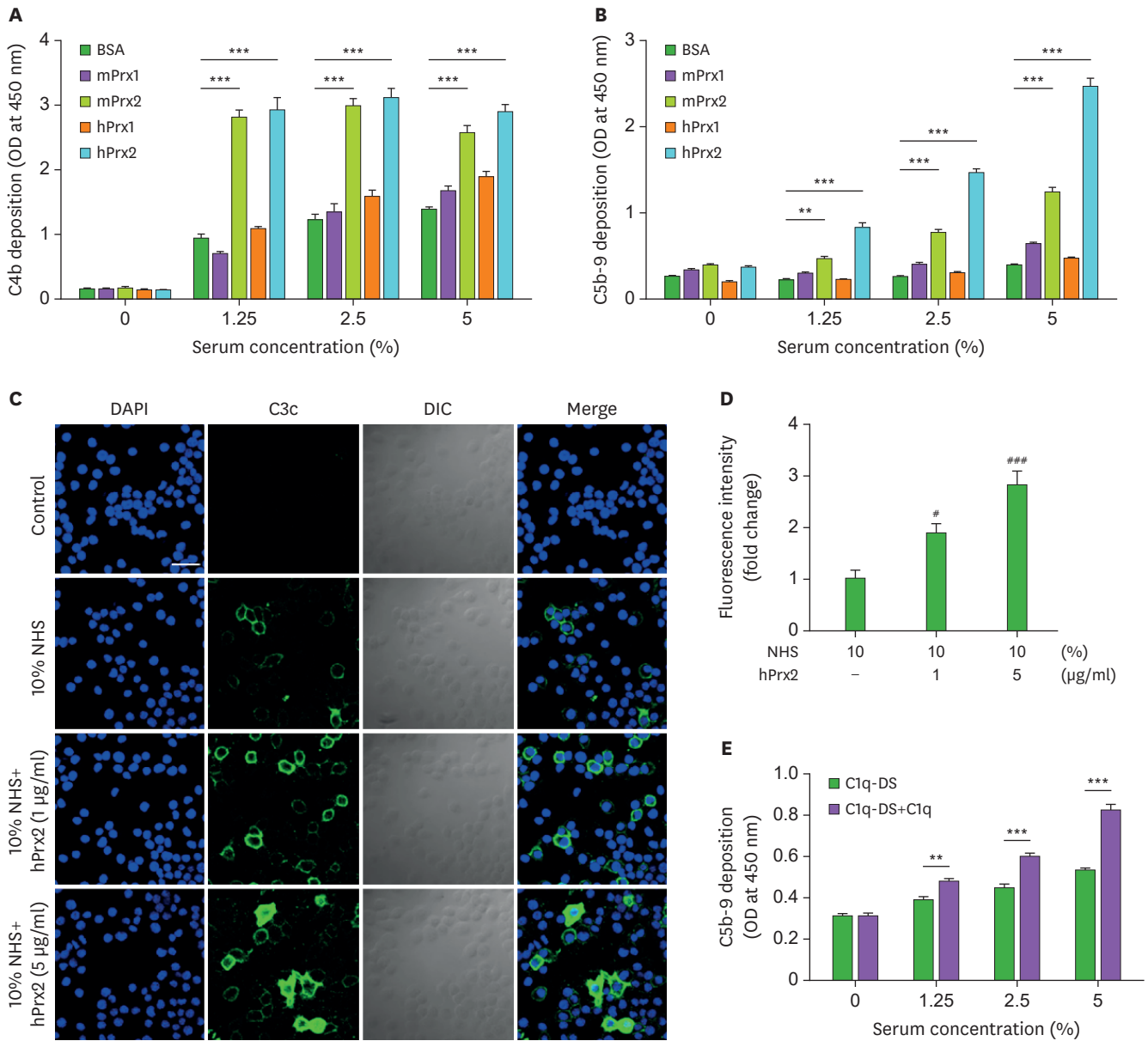


Figure 4. Binding of Prx2 to C1q activates the classical complement pathway. Recombinant mPrx1, mPrx2, hPrx1, and hPrx2 proteins (1 µg/ml) were immobilized on a microtiter plate and incubated with various concentrations of NHS to measure the quantity of C4b (A) or C5b-9 (B) deposition using ELISA. (C) J774A.1 cells were incubated with 10% NHS in the absence or presence of 1 or 5 µg/ml hPrx2 at 37°C for 2 h. Immunofluorescence staining was performed with anti-C3c-FITC Ab (scale bar=50 µm). (D) The mean relative fluorescence intensity of four visual fields was calculated using ImageJ. Data are expressed as means±SEMs (n=4). (E) Recombinant hPrx2 protein (1 µg/ml) was immobilized on a microtiter plate and incubated with various concentrations of C1q-depleted NHS (C1q-DS) or C1q-reconstituted NHS (C1q-DS+C1q) to measure the amount of C5b-9 deposition. Data are expressed as means±SEMs (n=3). DIC, differential interference contrast. **p<0.01, ***p<0.001 as Student's paired t-test (A, B, and E). *p<0.05, ***p<0.001 vs. 10% NHS in the absence of hPrx2 using one-way ANOVA with Bonferroni correction (D).

microscopy. J774A.1 cells were treated with 10% NHS in the absence or presence of 1 or 5 µg/ml hPrx2, and C3c was detected using an anti-C3c Ab conjugated with FITC. Treatment with 10% NHS and hPrx2 induced more C3c deposition on the J774A.1 cells than did the treatment with 10% NHS in the absence of hPrx2 (Fig. 4C). The relative values of fluorescence intensity were 1.90 and 2.83 in the presence of 1 and 5 µg/ml hPrx2, respectively, compared with that on treatment with 10% NHS in the absence of hPrx2 (Fig. 4D). Moreover, we tested whether

Prx2 induces the activation of the complement pathway in a C1q-dependent manner using C1q-depleted serum. Increasing concentrations of C1q-depleted NHS or C1q-reconstituted NHS were added to hPrx2-coated plates, and anti-C5b-9 Ab was added to observe the accumulation of C5b-9. C1q-reconstituted NHS induced C5b-9 deposition in an NHS concentration-dependent manner and showed more C5b-9 deposition than that induced by C1q-depleted NHS (Fig. 4E).

Complement is consumed by Prx2

We performed a complement consumption assay to verify our hypothesis that the hemolytic activity of complement could be mediated by hPrx2. Various concentrations of hPrx2 were pre-incubated with CH₅₀ NHS, after which Ab-sensitized sheep erythrocytes were added to measure the residual complement lytic activity. The aggregated IgG was used as a positive control. The complement consumption induced by hPrx2 increased in a concentration-dependent manner. The levels of complement consumption were 19.7% and 30.5% in the presence of 15 and 30 µg/ml hPrx2, respectively (Fig. 5). This result suggests that hPrx2 activates the hemolytic activity of the complement.

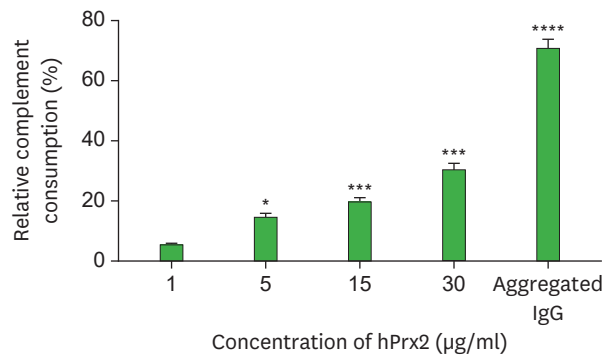


Figure 5. Complement is consumed by Prx2.

Various concentrations of the recombinant hPrx2 protein were incubated with diluted NHS containing CH₅₀ activity at 37°C for 30 min. After complement consumption by hPrx2, Ab-sensitized sheep erythrocytes were added in the consumed NHS at 37°C for 30 min. Aggregated IgG was used as a positive control. Data are expressed as means±SEMs (n=3). *p<0.05, ***p<0.001 vs. 1 µg/ml hPrx2 using one-way ANOVA with Bonferroni correction. ****p<0.001 vs. 30 µg/ml hPrx2 as Student's paired t-test.

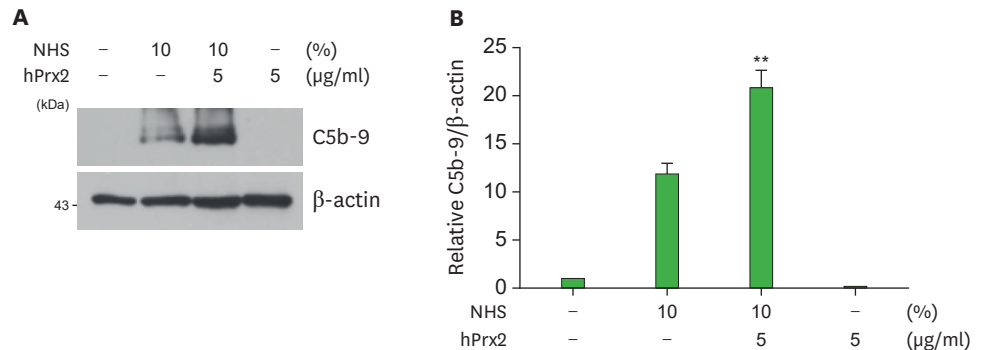


Figure 6. Prx2 increases C5b-9 deposition on murine macrophage.

(A) J774A.1 cells were treated with 10% NHS in the absence or presence of 5 µg/ml hPrx2, and WCLs were subjected to SDS-PAGE and immunoblotting. (B) Densitometric analysis of immunoblots was used to estimate the relative abundance of C5b-9 normalized to that of β-actin. Data are expressed as means±SEMs (n=3). **p<0.01 vs. 10% NHS only using one-way ANOVA with Bonferroni correction.

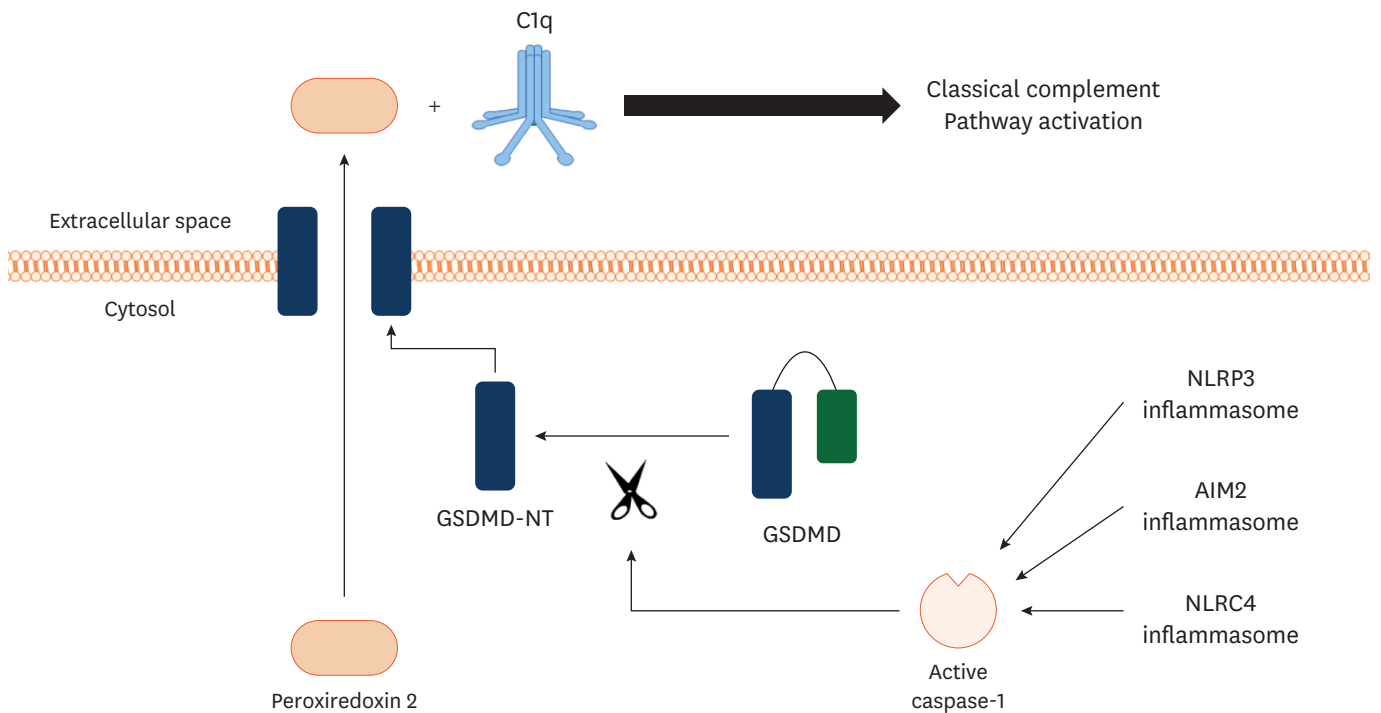


Figure 7. A model of Prx2 secretion and Prx2-mediated classical complement pathway activation. Upon inflammasome activation, active caspase-1 cleaves GSDMD. Cleavage of GSDMD results in GSDMD-NT; GSDMD-NT form pore on the plasma membrane; Prx2 is released through GSDMD pores; the released Prx2 binds with C1q and activates the classical complement pathway.

Prx2 increases C5b-9 deposition on the cell membrane of murine macrophage.

So far, we have shown that Prx2 binds with C1q, and the binding induces activation of the classical complement pathway. We next tested whether components of complement pathway activation induced by Prx2 could be accumulated on cells. J774A.1 cells were treated with 10% NHS in the absence or presence of 5 µg/ml hPrx2, and C5b-9 was detected by immunoblotting of WCLs. C5b-9 deposition on J774A.1 could be observed in the presence of 10% NHS, and this deposition was intensified with the addition of 5 µg/ml hPrx2. Whereas hPrx2 itself, in the absence of 10% NHS, showed no detection of C5b-9 deposition on J774A.1 (Fig. 6A and B). A model of Prx2 secretion and Prx2-mediated classical complement pathway activation is summarized in Fig. 7.

DISCUSSION

Prxs are well-known antioxidant proteins that scavenge peroxides in cells. In this aspect, many studies demonstrated that Prxs could play a protective role in diverse disease models (24-28). Recent evidence has suggested that Prxs could possibly act as DAMP molecules mediating the secretion of inflammatory cytokines as shown in various disease models (1,6-8). To be referred to as a DAMP molecule, a certain molecule should be released upon cellular stress or tissue injury and should induce inflammation by triggering the innate immune response (29). In previous studies regarding the role of Prxs in the context of inflammation, released Prxs induced expression and secretion of inflammatory cytokines from inflammatory cells and were associated with tissue damage in multiple disease models. Particularly, Prxs released from necrotic brain cells induced IL-1β, IL-23, and TNF-α

expression in macrophages through activation of TLR2 and TLR4, and Prx1 released in the context of acute liver injury induced IL-1 β , IL-6, and TNF- α production from macrophages through NF- κ B and NLRP3 inflammasome signaling (6,8). However, these studies only described the effect of released Prxs on the inflammatory response, whereas the mechanism through which release of Prxs occurs was not mentioned or investigated. And these studies focused on the expression or secretion of inflammatory cytokines and tissue damage induced by released Prxs, whereas the effect of released Prxs on activation of the complement system remains to be elucidated (6-8).

In this study, we showed that inflammasome activation could be a mechanism triggering the release of Prxs, and GSDMD pore formation could be the route allowing the release of the Prxs. Conventionally, inflammasome activation and subsequent formation of the GSDMD pores have been mainly associated with the release of IL-1 β , IL-18, and several DAMP molecules such as HMGB1, DNA, and ATP (10,30). Recently, several studies have suggested the association between released Prxs and inflammasome activation, showing that the released Prxs could induce inflammasome activation and secretion of IL-1 β (6,8). However, the hypothesis that inflammasome activation could induce the release of Prxs has not been elucidated. Based on these data, we propose that various Prxs are released upon inflammasome activation in a caspase-1 dependent manner, and GSDMD pore could be a mediator of the Prx release. Specifically, Prx1, Prx2, Prx5, and Prx6 are released upon inflammasome activation in a caspase-1-dependent manner among the 6 types of Prxs. Differential distribution of various Prxs in the intracellular compartment may be a reason why different release patterns exist according to the type of Prxs upon inflammasome activation (1). A few studies have investigated the role of Prxs as a DAMP molecule in the context of various disease models. However, they did not suggest the secretory mechanism of Prxs (6-8). In this aspect, our findings provide novel insight into Prxs as DAMP molecules.

We observed that the mouse and human forms of Prx1 and Prx2 could bind with C1q, and the binding of C1q with Prx2, but not with Prx1, could induce the activation of the classical complement pathway, resulting in C5b-9 deposition. The classical complement pathway is activated by C1q binding with Ag-Ab complexes or binding with the PTX3 family of plasma proteins such as C-reactive protein, amyloid protein, and PTX3 (31), and as recently revealed, with HMGB1 (17). These findings, along with our data, suggest that Prx2 may be another ligand of C1q that may be capable of Ab-independent activation of the classical complement pathway; extracellular secretion of Prx2 by inflammasome activation could induce further inflammatory responses via activation of the classical complement pathway. However, further investigation is necessary to determine the detailed mechanism of C1q binding with Prx2 in a specific disease model and the subsequent classical complement pathway activation and functional role of C1q binding with Prx1.

Activation of the complement pathway results in cell lysis or tissue damage by MAC, the terminal effector of the complement pathway. However, there are multiple recovery or resistance mechanisms against the cell lytic activity of MAC. In the presence of these recovery or resistance mechanisms, a sub-lytic or non-lethal dose of MAC induces various biological responses (32,33). For instance, in inflammatory cells, sub-lytic or non-lethal doses of MAC could trigger the synthesis and release of proinflammatory mediators, such as reactive oxygen metabolites, metabolites of arachidonic acid including prostaglandins, thromboxanes, and leukotrienes, and inflammatory cytokines via the activation of several signaling pathways, including MAPK, protein kinase C, and NF- κ B pathway (33-36). In our study, treatment with

hPrx2 and NHS resulted in a significantly higher amount of C5b-9 deposition on the J774A.1 cells compared to that on treatment with NHS in the absence of hPrx2. These findings imply that extracellular Prx2 could induce further inflammatory responses mediated by the sub-lytic effect of C5b-9.

Recently, emerging evidence has suggested that inflammatory components exist in diverse cancers, metabolic disorders, cardiovascular diseases, and neurodegenerative diseases (37-40). Inflammasome is a frequently researched area among the various inflammatory processes related to diverse diseases. Atherosclerosis, diabetes mellitus, Parkinson's disease, and Alzheimer's disease are typical diseases in which inflammasomes play a critical role in the initiation and progression of the disease (41). In this regard, our results suggest that Prx2 could be secreted and amplify tissue injury mediated by the classical complement pathway in inflammasome-related diseases; therefore, blocking Prx2 may have therapeutic implications in those diseases.

In summary, our results suggest that inflammasome activation is possibly a secretory mechanism of Prxs, and GSDMD is a mediator for the secretion of Prxs. The secreted Prx1 and Prx2 can bind with C1q; however, only the secreted Prx2 can activate the classical complement pathway in a C1q-dependent manner. These results imply that Prx2 could be a therapeutic target in many inflammasome-related diseases.

ACKNOWLEDGEMENTS

We thank Sook Young Kim for the help of complement-related assay. This work was supported by grants from the National Research Foundation of Korea (NRF) funded by the Korean government (No. 2017R1A2B3006704, 2019R1A6A1A03032869, 2021R1H1A1A01044809).

SUPPLEMENTARY MATERIAL

Supplementary Figure 1

Inflammasomes mediated Prx1 and Prx2 secretion from BMDMs and J774A.1 cells.

[Click here to view](#)

REFERENCES

1. Cox AG, Winterbourn CC, Hampton MB. Mitochondrial peroxiredoxin involvement in antioxidant defence and redox signalling. *Biochem J* 2009;425:313-325.
[PUBMED](#) | [CROSSREF](#)
2. Lee S, Wi SM, Min Y, Lee KY. Peroxiredoxin-3 is involved in bactericidal activity through the regulation of mitochondrial reactive oxygen species. *Immune Netw* 2016;16:373-380.
[PUBMED](#) | [CROSSREF](#)
3. Neumann CA, Krause DS, Carman CV, Das S, Dubey DP, Abraham JL, Bronson RT, Fujiwara Y, Orkin SH, Van Etten RA. Essential role for the peroxiredoxin Prdx1 in erythrocyte antioxidant defence and tumour suppression. *Nature* 2003;424:561-565.
[PUBMED](#) | [CROSSREF](#)

4. Lee TH, Kim SU, Yu SL, Kim SH, Park DS, Moon HB, Dho SH, Kwon KS, Kwon HJ, Han YH, et al. Peroxiredoxin II is essential for sustaining life span of erythrocytes in mice. *Blood* 2003;101:5033-5038.
[PUBMED](#) | [CROSSREF](#)
5. Perricone C, De Carolis C, Perricone R. Glutathione: a key player in autoimmunity. *Autoimmun Rev* 2009;8:697-701.
[PUBMED](#) | [CROSSREF](#)
6. Shichita T, Hasegawa E, Kimura A, Morita R, Sakaguchi R, Takada I, Sekiya T, Ooboshi H, Kitazono T, Yanagawa T, et al. Peroxiredoxin family proteins are key initiators of post-ischemic inflammation in the brain. *Nat Med* 2012;18:911-917.
[PUBMED](#) | [CROSSREF](#)
7. Salzano S, Checconi P, Hanschmann EM, Lillig CH, Bowler LD, Chan P, Vaudry D, Mengozzi M, Coppo L, Sacre S, et al. Linkage of inflammation and oxidative stress via release of glutathionylated peroxiredoxin-2, which acts as a danger signal. *Proc Natl Acad Sci U S A* 2014;111:12157-12162.
[PUBMED](#) | [CROSSREF](#)
8. He Y, Li S, Tang D, Peng Y, Meng J, Peng S, Deng Z, Qiu S, Liao X, Chen H, et al. Circulating peroxiredoxin-1 is a novel damage-associated molecular pattern and aggravates acute liver injury via promoting inflammation. *Free Radic Biol Med* 2019;137:24-36.
[PUBMED](#) | [CROSSREF](#)
9. Schroder K, Tschopp J. The inflammasomes. *Cell* 2010;140:821-832.
[PUBMED](#) | [CROSSREF](#)
10. Feng S, Fox D, Man SM. Mechanisms of gasdermin family members in inflammasome signaling and cell death. *J Mol Biol* 2018;430:3068-3080.
[PUBMED](#) | [CROSSREF](#)
11. Ding J, Wang K, Liu W, She Y, Sun Q, Shi J, Sun H, Wang DC, Shao F. Pore-forming activity and structural autoinhibition of the gasdermin family. *Nature* 2016;535:111-116.
[PUBMED](#) | [CROSSREF](#)
12. Liu X, Zhang Z, Ruan J, Pan Y, Magupalli VG, Wu H, Lieberman J. Inflammasome-activated gasdermin D causes pyroptosis by forming membrane pores. *Nature* 2016;535:153-158.
[PUBMED](#) | [CROSSREF](#)
13. Walport MJ. Complement. First of two parts. *N Engl J Med* 2001;344:1058-1066.
[PUBMED](#) | [CROSSREF](#)
14. Walport MJ. Complement. Second of two parts. *N Engl J Med* 2001;344:1140-1144.
[PUBMED](#) | [CROSSREF](#)
15. Païdassi H, Tacnet-Delorme P, Garlatti V, Darnault C, Ghebrehiwet B, Gaboriaud C, Arlaud GJ, Frchet P. C1q binds phosphatidylserine and likely acts as a multiligand-bridging molecule in apoptotic cell recognition. *J Immunol* 2008;180:2329-2338.
[PUBMED](#) | [CROSSREF](#)
16. Kang YH, Tan LA, Carroll MV, Gentle ME, Sim RB. Target pattern recognition by complement proteins of the classical and alternative pathways. *Adv Exp Med Biol* 2009;653:117-128.
[PUBMED](#) | [CROSSREF](#)
17. Kim SY, Son M, Lee SE, Park IH, Kwak MS, Han M, Lee HS, Kim ES, Kim JY, Lee JE, et al. High-mobility group box 1-induced complement activation causes sterile inflammation. *Front Immunol* 2018;9:705.
[PUBMED](#) | [CROSSREF](#)
18. Hornung V, Bauernfeind F, Halle A, Samstad EO, Kono H, Rock KL, Fitzgerald KA, Latz E. Silica crystals and aluminum salts activate the NALP3 inflammasome through phagosomal destabilization. *Nat Immunol* 2008;9:847-856.
[PUBMED](#) | [CROSSREF](#)
19. Kaplan MH, Volanakis JE. Interaction of C-reactive protein complexes with the complement system. I. Consumption of human complement associated with the reaction of C-reactive protein with pneumococcal C-polysaccharide and with the choline phosphatides, lecithin and sphingomyelin. *J Immunol* 1974;112:2135-2147.
[PUBMED](#)
20. Bhakdi S, Torzewski M, Paprotka K, Schmitt S, Barsoom H, Suriyaphol P, Han SR, Lackner KJ, Husmann M. Possible protective role for C-reactive protein in atherogenesis: complement activation by modified lipoproteins halts before detrimental terminal sequence. *Circulation* 2004;109:1870-1876.
[PUBMED](#) | [CROSSREF](#)
21. Shi J, Zhao Y, Wang K, Shi X, Wang Y, Huang H, Zhuang Y, Cai T, Wang F, Shao F. Cleavage of GSDMD by inflammatory caspases determines pyroptotic cell death. *Nature* 2015;526:660-665.
[PUBMED](#) | [CROSSREF](#)

22. Kayagaki N, Stowe IB, Lee BL, O'Rourke K, Anderson K, Warming S, Cuellar T, Haley B, Roose-Girma M, Phung QT, et al. Caspase-11 cleaves gasdermin D for non-canonical inflammasome signalling. *Nature* 2015;526:666-671.
[PUBMED](#) | [CROSSREF](#)
23. He WT, Wan H, Hu L, Chen P, Wang X, Huang Z, Yang ZH, Zhong CQ, Han J. Gasdermin D is an executor of pyroptosis and required for interleukin-1 β secretion. *Cell Res* 2015;25:1285-1298.
[PUBMED](#) | [CROSSREF](#)
24. Jeong SJ, Kim S, Park JG, Jung IH, Lee MN, Jeon S, Kweon HY, Yu DY, Lee SH, Jang Y, et al. Prdx1 (peroxiredoxin 1) deficiency reduces cholesterol efflux via impaired macrophage lipophagic flux. *Autophagy* 2018;14:120-133.
[PUBMED](#) | [CROSSREF](#)
25. Jeong SJ, Cho MJ, Ko NY, Kim S, Jung IH, Min JK, Lee SH, Park JG, Oh GT. Deficiency of peroxiredoxin 2 exacerbates angiotensin II-induced abdominal aortic aneurysm. *Exp Mol Med* 2020;52:1587-1601.
[PUBMED](#) | [CROSSREF](#)
26. Wang Y, Zhao Y, Wang Z, Sun R, Zou B, Li R, Liu D, Lin M, Zhou J, Ning S, et al. Peroxiredoxin 3 inhibits acetaminophen-induced liver pyroptosis through the regulation of mitochondrial ROS. *Front Immunol* 2021;12:652782.
[PUBMED](#) | [CROSSREF](#)
27. Nabeshima A, Yamada S, Guo X, Tanimoto A, Wang KY, Shimajiri S, Kimura S, Tasaki T, Noguchi H, Kitada S, et al. Peroxiredoxin 4 protects against nonalcoholic steatohepatitis and type 2 diabetes in a nongenetic mouse model. *Antioxid Redox Signal* 2013;19:1983-1998.
[PUBMED](#) | [CROSSREF](#)
28. Kim MH, Seong JB, Huh JW, Bae YC, Lee HS, Lee DS. Peroxiredoxin 5 ameliorates obesity-induced non-alcoholic fatty liver disease through the regulation of oxidative stress and AMP-activated protein kinase signaling. *Redox Biol* 2020;28:101315.
[PUBMED](#) | [CROSSREF](#)
29. Roh JS, Sohn DH. Damage-associated molecular patterns in inflammatory diseases. *Immune Netw* 2018;18:e27.
[PUBMED](#) | [CROSSREF](#)
30. Gim E, Shim DW, Hwang I, Shin OS, Yu JW. Zika virus impairs host NLRP3-mediated inflammasome activation in an NS3-dependent manner. *Immune Netw* 2019;19:e40.
[PUBMED](#) | [CROSSREF](#)
31. Kishore U, Gaboriaud C, Waters P, Shrive AK, Greenhough TJ, Reid KB, Sim RB, Arlaud GJ. C1q and tumor necrosis factor superfamily: modularity and versatility. *Trends Immunol* 2004;25:551-561.
[PUBMED](#) | [CROSSREF](#)
32. Wang Q, Rozelle AL, Lepus CM, Scanzello CR, Song JJ, Larsen DM, Crish JF, Bebek G, Ritter SY, Lindstrom TM, et al. Identification of a central role for complement in osteoarthritis. *Nat Med* 2011;17:1674-1679.
[PUBMED](#) | [CROSSREF](#)
33. Bohana-Kashtan O, Ziporen L, Donin N, Kraus S, Fishelson Z. Cell signals transduced by complement. *Mol Immunol* 2004;41:583-597.
[PUBMED](#) | [CROSSREF](#)
34. Morgan BP. Complement membrane attack on nucleated cells: resistance, recovery and non-lethal effects. *Biochem J* 1989;264:1-14.
[PUBMED](#) | [CROSSREF](#)
35. Stahl RA, Adler S, Baker PJ, Chen YP, Pritzl PM, Couser WG. Enhanced glomerular prostaglandin formation in experimental membranous nephropathy. *Kidney Int* 1987;31:1126-1131.
[PUBMED](#) | [CROSSREF](#)
36. Hänsch GM, Seitz M, Betz M. Effect of the late complement components C5b-9 on human monocytes: release of prostanoids, oxygen radicals and of a factor inducing cell proliferation. *Int Arch Allergy Appl Immunol* 1987;82:317-320.
[PUBMED](#) | [CROSSREF](#)
37. Ruparelina N, Chai JT, Fisher EA, Choudhury RP. Inflammatory processes in cardiovascular disease: a route to targeted therapies. *Nat Rev Cardiol* 2017;14:133-144.
[PUBMED](#) | [CROSSREF](#)
38. Wyss-Coray T, Mucke L. Inflammation in neurodegenerative disease--a double-edged sword. *Neuron* 2002;35:419-432.
[PUBMED](#) | [CROSSREF](#)
39. Hotamisligil GS. Inflammation and metabolic disorders. *Nature* 2006;444:860-867.
[PUBMED](#) | [CROSSREF](#)

40. Coussens LM, Werb Z. Inflammation and cancer. *Nature* 2002;420:860-867.
[PUBMED](#) | [CROSSREF](#)
41. Guo H, Callaway JB, Ting JP. Inflammasomes: mechanism of action, role in disease, and therapeutics. *Nat Med* 2015;21:677-687.
[PUBMED](#) | [CROSSREF](#)